The Astrophysical Journal Supplement Series, 164:124–129, 2006 May

MARS ODYSSEY JOINS THE THIRD INTERPLANETARY NETWORK

K. Hurley
University of California, Berkeley, Space Sciences Laboratory, 7 Gauss Way, Berkeley, CA 94720-7450; khurley@ssl.berkeley.edu

I. Mitrofanov, A. Kozyrev, M. Litvak, A. Sanin V. Grinkov, and S. Charyshnikov
Institute for Space Research, Moscow 117810, Russia

W. Boynton, C. Fellows, K. Harshman, D. Hamara, and C. Shinohara
Lunar and Planetary Laboratory, University of Arizona, 1629 East University Boulevard, Tucson, AZ 85721-0092

R. Starr
The Catholic University of America, Department of Physics, Washington, DC 20064

and

T. Cline
NASA Goddard Space Flight Center, Code 661, Greenbelt, MD 20771
Received 2005 September 8; accepted 2006 January 16

ABSTRACT

The *Mars Odyssey* spacecraft carries two experiments that are capable of detecting cosmic gamma-ray bursts and soft gamma repeaters. Since 2001 April they have detected over 275 bursts and, in conjunction with the other spacecraft of the interplanetary network, localized many of them rapidly and precisely enough to allow sensitive multiwavelength counterpart searches. We present the *Mars Odyssey* mission and describe the burst capabilities of the two experiments in detail. We explain how the spacecraft timing and ephemeris have been verified in-flight using bursts from objects whose precise positions are known by other means. Finally, we show several examples of localizations and discuss future plans for the *Odyssey* mission and the network as a whole.

Subject headings: catalogs — gamma rays: bursts

1. INTRODUCTION

Interplanetary networks (IPNs) have played an important role in the studies of both cosmic gamma-ray bursts (GRBs) and soft gamma repeaters (SGRs) for over two decades. Indeed, until the launch of *BeppoSAX* in 1996, the only way to derive arcminute positions for these objects was by comparing their arrival times at distant spacecraft. The current (third) IPN was formed when the *Ulysses* spacecraft was launched in 1990. Over 25 spacecraft have participated in the IPN since then, and the latest interplanetary mission to join the network is *Mars Odyssey*. It seems fitting that this spacecraft should belong to the IPN, since "Odyssey" and "Ulysses" both refer to the same saga of distant voyages. Today, the IPN comprises the *Ulysses*, Konus-*Wind*, *RHESSI*, *High Energy Transient Explorer* (*HETE*), *International Gamma-Ray Astrophysics Laboratory* (*INTEGRAL*), *Swift*, and *Mars Odyssey* (*MO*) missions and experiments, and, with a detection rate of 200 events per year, is responsible for most GRB and SGR detections and localizations. As a distant point in the network, *MO* plays a crucial role: without it, only localizations to annuli or large error boxes would be possible. The triangulation or arrival-time analysis method for localizing bursts has been presented elsewhere (Hurley et al. 1999a, 1999b). In this paper, we concentrate on the properties of the two *MO* experiments that make burst detection possible. We note that this is the fifth attempt, and the first successful one, to place a GRB detector in Mars orbit; the four previous attempts, on board the *Phobos 1* and *2* (Sagdeev & Zakharov 1990), *Mars Observer* (Metzger et al. 1992), and *Mars '96* (Ziock et al. 1997) missions, met with limited or no success due to mission failures.

2. THE *MARS ODYSSEY* MISSION

The *Mars Odyssey* mission is an orbiter whose objective is to provide a better understanding of the climate and geologic history of Mars. It was launched on 2001 April 7, and after a 6 month cruise phase, reached Mars on 2001 October 24. The mission then entered an aerobraking phase to circularize the orbit that lasted until 2002 January. At the end of this phase, the spacecraft was orbiting the planet every 1.964 hr at an altitude between 370 and 432 km (Saunders et al. 2004). The prime scientific mission then commenced, and at present, *Odyssey* is in its first extended mission, which will continue through 2006 September; a mission extension beyond that date is likely.

The spacecraft is shown in Figure 1. In its present orbit, Mars subtends approximately 27% of the sky (62° half-angle) at the Odyssey spacecraft. In general, the instruments are powered on continuously, and almost 100% of the data are downlinked through the Deep Space Network during daily tracking passes. A more complete description of the mission has appeared in Saunders et al. (2004).

2.1. *The Gamma Sensor Head and the High Energy Neutron Detector*

The Gamma-Ray Spectrometer (GRS) is an instrument suite that includes two detectors with GRB detection capabilities, the gamma sensor head (GSH), and the High Energy Neutron Detector (HEND). The principal objective of the GRS experiment is the determination of the elemental abundances on Mars. The GSH consists of a 6.7 cm diameter times 6.7 cm high (cross-sectional area to GRBs $\sim$40 cm^2) right circular cylindrical germanium detector that is passively cooled and mounted on a boom extending 6 m from the body of the spacecraft. It records energy spectra between $\sim$50 keV and 10 MeV in a low time resolution mode ($\sim$20 s) until triggered by a burst. It then records GRB time histories in a single energy channel with 32 ms resolution for 19.75 s and can retrigger immediately thereafter. The

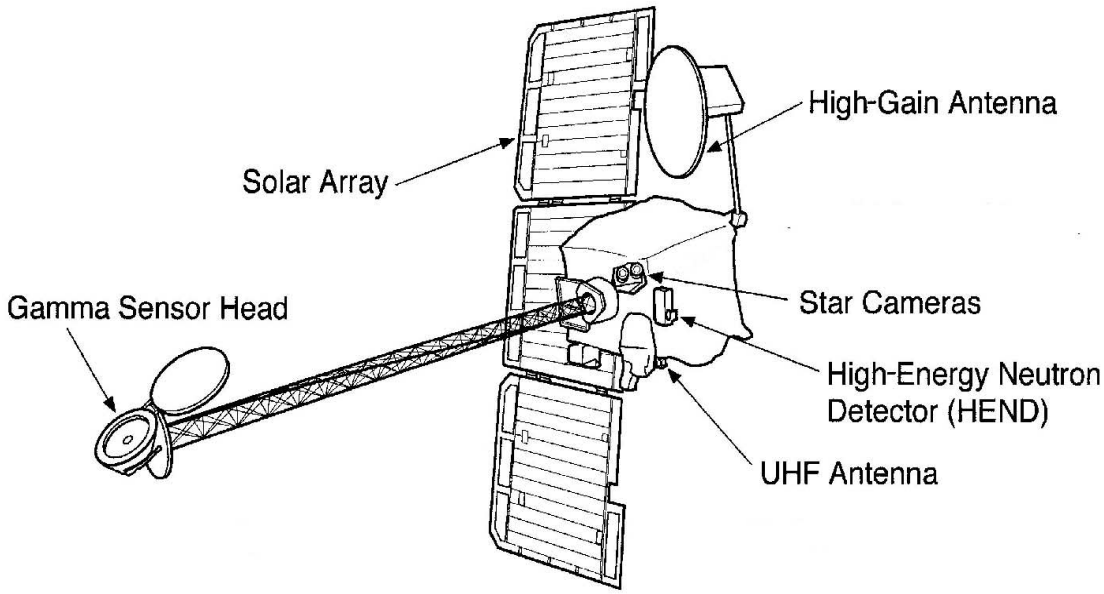

FIG. 1.—*Mars Odyssey* spacecraft, showing the positions of the HEND and GSH experiments, on the body of the spacecraft and on the boom, respectively.

boom extension and detector cooling did not take place until after the end of the aerobraking phase, and thus the experiment did not collect useful GRB data until then. The in-orbit background rate is $\sim$100 counts s^{-1} in the GRB energy channel, but it undergoes variations due to numerous causes. In order of decreasing importance, these are (1) the albedo from the cosmic gamma-ray background from the Martian surface, which is different for different regions of the planet, (2) seasonal changes on $\sim$month timescales such as CO_2 condensation in the polar cap regions (which suppresses the upcoming gamma-radiation from the surface of the planet), and (3) solar proton events. The GSH is shown in Figure 2. More details may be found in Boynton et al. (2004).

The burst detection portion of the HEND experiment is based on two optically separate scintillation detectors (Fig. 3). The first is a cylindrical stilbene crystal with a diameter of 30 mm and a height of 40 mm, which is used for the detection of high-energy neutrons and records gamma-rays as a by-product. These counts are measured continuously in the 350–3000 keV range with a time resolution of 1 s. The second detector is a cylindrical CsI(Tl) anticoincidence well surrounding the stilbene, whose thickness is 10 mm, whose outer diameter is 50 mm, and whose height is 49 mm. Thus, its cross-sectional area to GRBs varies between 19.6 cm^2 (on-axis), 24.5 cm^2 (90° off-axis), and 7.1 cm^2 (180° off-axis, counting the annular part only). The limiting sensitivity is about 10^{-6} erg cm^{-2}. In triggered mode, counts from the CsI are recorded in the $\sim$30–1300 keV energy range with a time resolution of 250 ms, and these data are used for triangulation. The upper and lower energy limits are only approximate, since the

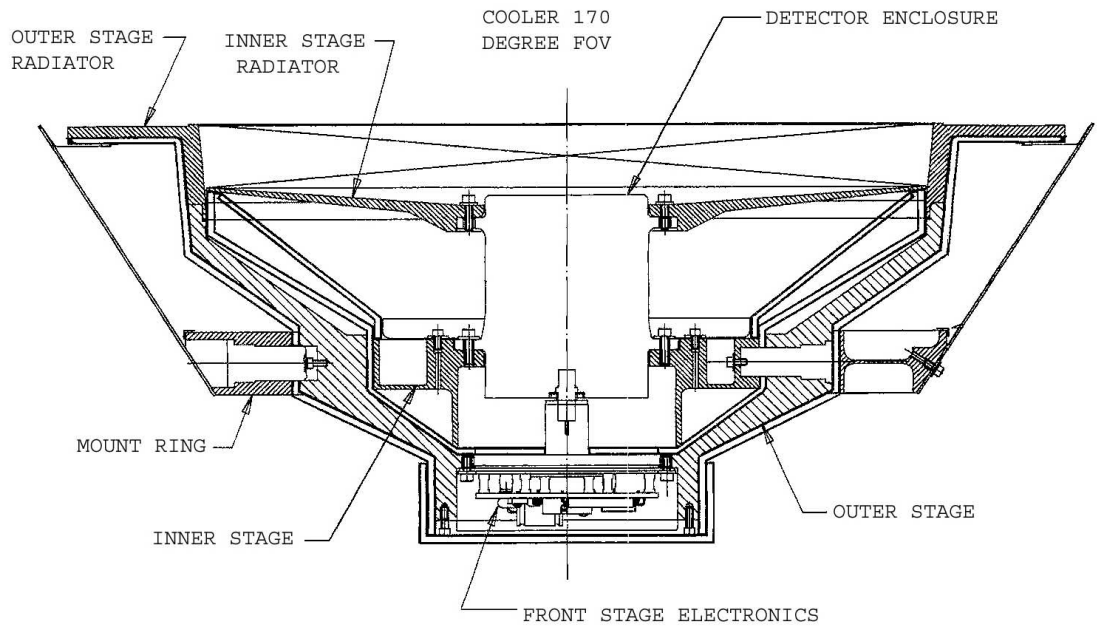

FIG. 2.—Cross section of the gamma sensor head, showing the germanium detector and the cooler. The upper part of the head faces into space, and Mars is toward the bottom.

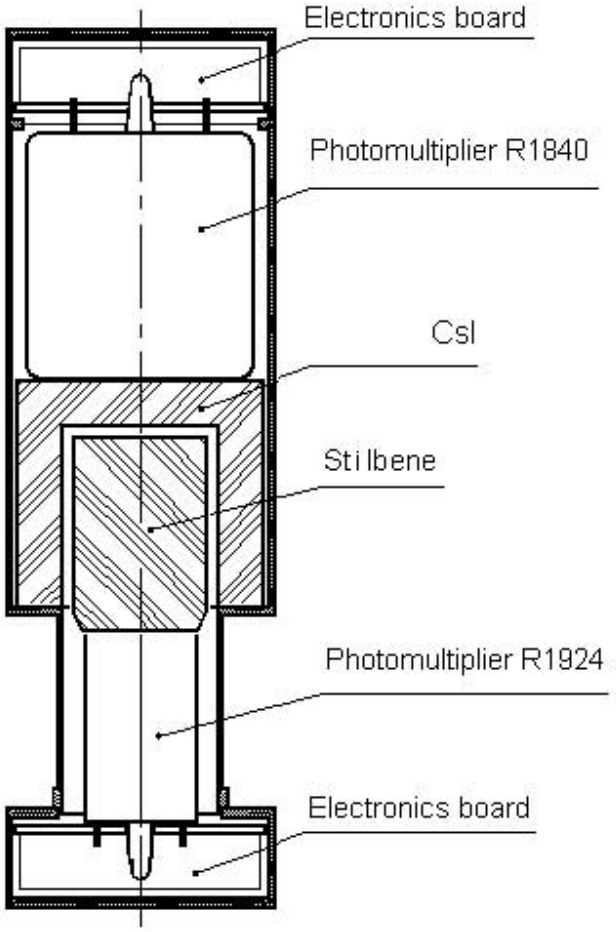

FIG. 3.—High Energy Neutron Detector (HEND) experiment. The detector axis points toward the top of the figure and is indicated by the center line. In the orbital phase of the mission, it points toward the nadir, that is, toward the surface of Mars.

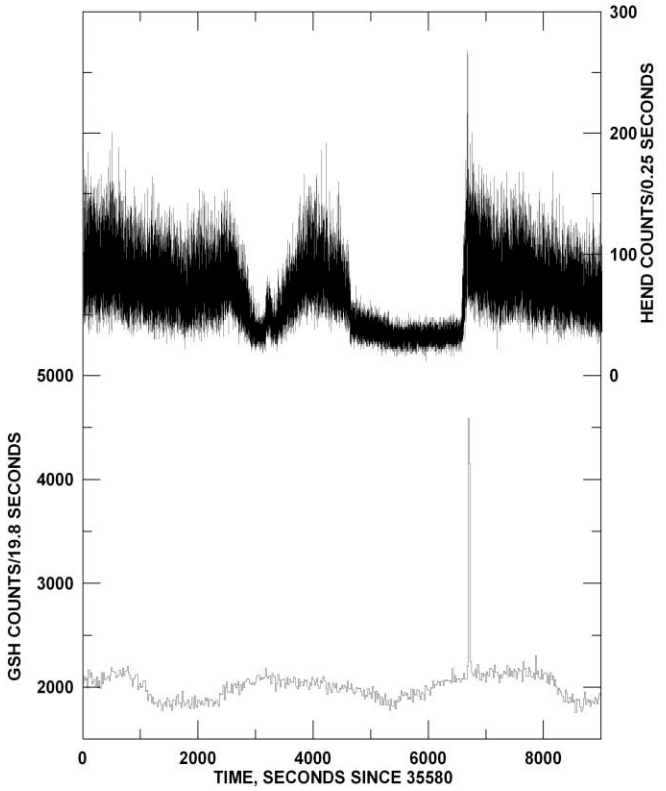

FIG. 4.—A ~9000 s (1.27 orbits) plot of the GSH (*bottom, left-hand axis*) and HEND (*top, right-hand axis*) counting rates on 2003 March 29, starting at 35,580 s). A bright gamma-ray burst occurred around 6600 s.

light collection in the cylindrical crystal depends on the photon interaction point. Energy spectra are not transmitted. The capacity of the counters is limited to 511 counts every 250 ms, so very strong bursts can temporarily saturate the detector. HEND is mounted on the body of the spacecraft. The in-orbit background rates are ~5 counts s^{-1} for the inner stilbene detector, and ~130 counts s^{-1} for the CsI anticoincidence. Both these rates undergo variations for the same reasons as the GSH, and in addition, because of HEND's lower energy threshold, due to trapped particles. For example, for a period of approximately 7 months starting on 2002 November 11, the background variations along the orbit increased from their nominal value of about a factor of 2 to a factor of 30. The cause of this increase is suspected to be trapped particles. During this time, the duty cycle for GRB detection decreased by a factor of 3.4. These large variations disappeared around 2003 June 9. Occasionally, they reappear rather reduced in strength. A background plot is shown in Figure 4. More details of the instrument may be found in Boynton et al. (2004).

3. BURST DETECTION AND STATISTICS

Bursts are detected in HEND and the GSH in different ways. HEND is equipped with an on-board trigger, but the telemetry allocation made it possible to transmit triggered data continuously. Thus, the trigger level was set to a value below the background level, and in effect, the experiment triggers continuously and produces continuous data with 250 ms time resolution. Searches for bursts in the HEND data may therefore be initiated by detections on other IPN spacecraft and may be carried out in the ground analysis. Every candidate event detected by an IPN spacecraft initiates such a search, and almost all the bursts detected by HEND to date have been found by searching the data in the crossing time window that corresponds to these candidate events. (Thus, for example, in the case of an event detected by *Ulysses*, the crossing time window is the Mars-*Ulysses* distance expressed in light-seconds; the maximum distance is ~3000 lt-s.) Up to now, no exhaustive automatic "blind" search for bursts has been carried out in the HEND data, although an algorithm to do this is being developed and tested. GSH burst data, on the other hand, come only from on-board triggers; each trigger initiates a search for a confirming event in the data of the other IPN spacecraft in the appropriate crossing time windows. As high time resolution GSH data are only available for triggered events, it is usually not practical to search the data for bursts detected by other spacecraft.

HEND was turned on during the cruise phase and detected its first confirmed GRB on 2001 May 8. In the 1520 days that followed, HEND and/or GRS have detected >275 GRBs or SGRs that have been confirmed by detection on board at least one other IPN spacecraft. Thus, the average burst detection rate during the cruise and orbital phases is about one burst every 5.9 days. This number is an average over the entire period and does not take high background periods, or times when the experiments were turned off, into account. The true rate would therefore be higher. Initially, the spacecraft timing was not determined accurately during the

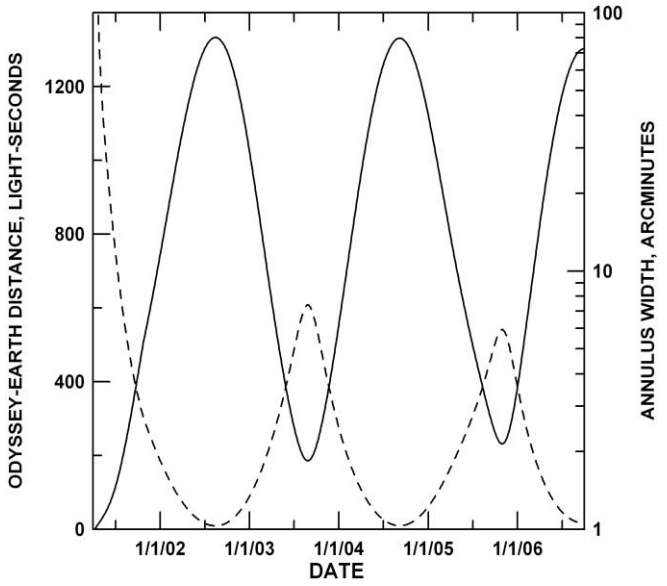

FIG. 5.—Typical width of an IPN annulus obtained by triangulation between *Mars Odyssey* and a near-Earth spacecraft, as a function of time, from 2001 April to the nominal end of mission (2006 October). The left-hand scale shows the *Odyssey* Earth distance in light-seconds (*solid line*), and the right-hand scale gives the annulus width in arcminutes (*dashed line*). A cross-correlation uncertainty of 200 ms and a GRB arrival angle 30° from the Mars-Earth vector have been assumed.

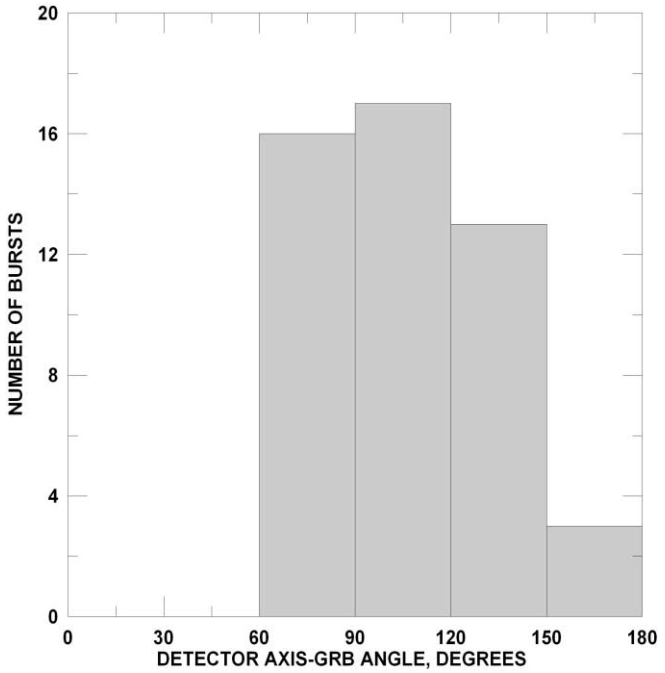

FIG. 6.—Angular distribution of GRBs detected by HEND during the orbital phase of the mission, relative to the detector axis. The detector axis is pointed toward Mars in the orbital phase, so no bursts are detected at angles less than roughly 60°. Around 180°, the relatively small detection cross section (see Fig. 3) and spacecraft-blocking reduce the number of detections.

cruise phase and no triangulation results were announced. (These data have since been reprocessed for accurate timing.) Thus, the *Odyssey* mission became most useful to the IPN when it entered its orbital phase; at that point its separation from Earth was large enough for the triangulation method to produce small error boxes, and the timing was known to good accuracy in real time. The typical IPN annulus width as a function of time over the mission is shown in Figure 5.

The GRB detection rate by three widely separated spacecraft (that is, *Mars Odyssey*, *Ulysses*, and any near-Earth mission) is about 1 every 7 days. It is interesting to note that this rate is identical to that which was obtained when the *Near Earth Asteroid Rendezvous* (*NEAR*) mission was the other distant spacecraft in addition to *Ulysses*. These numbers do not depend strongly on any comparison of the *MO* and *NEAR* instrument sensitivities, for the following reason. Due to its small size, *Ulysses* tends to be the least sensitive detector in the network. We are counting only those bursts that were detected by *Ulysses*, a near-Earth spacecraft, and another, distant spacecraft. As long as the sensitivities of the near-Earth and the distant spacecraft are greater than that of *Ulysses*, the burst rate is determined primarily by *Ulysses'* sensitivity, rather than by that of the other detectors.

Figure 6 presents the distribution of the angles between the HEND detector axis, which is always pointed toward Mars in the orbital phase of the mission, and the GRBs detected by it. This distribution agrees with the wide field of view of the CsI anticoincidence, which is limited mainly by the Mars horizon; the body of the spacecraft blocks a small fraction of the sky with relatively low atomic number materials.

Figure 7 compares the count rates for events detected by HEND and *Ulysses*. Since the HEND count rate is roughly proportional to that of *Ulysses*, this relation can be used for an approximate estimate of the fluence of HEND bursts. The weakest confirmed GRB detected by HEND to date had a fluence of about 1.5×10^{-6} erg cm^{-2}.

4. VERIFYING THE IPN RESULTS

Whenever a new spacecraft enters the network, both its timing and its ephemeris must be verified in-flight. There are various ways to do this, but the most effective end-to-end test is to triangulate bursts whose positions are known with greater precision

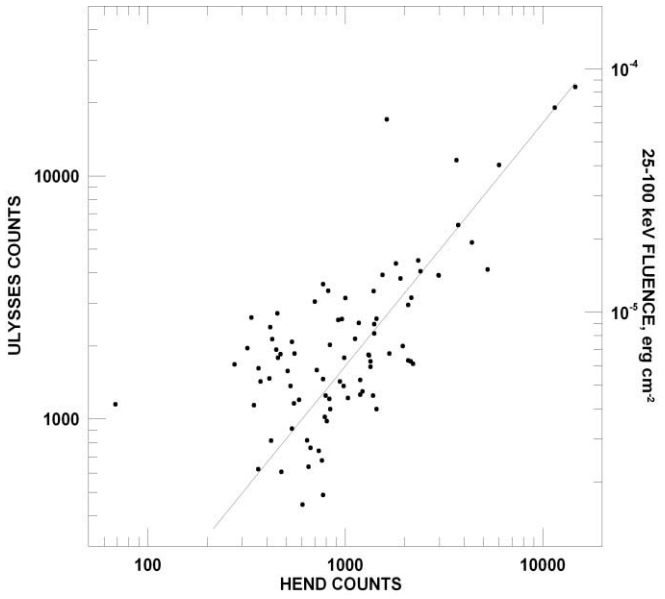

FIG. 7.—Integrated counts for 87 GRBs detected by *Ulysses* in the 25–150 keV energy range, vs. the integrated counts detected by HEND in the 30–1300 keV range. The *Ulysses* detector has an approximately isotropic response, while the HEND cross-sectional area varies considerably depending on the arrival direction. This, as well as the spectral differences between the bursts, explains much of the scatter in the points. However, the HEND counts are approximately equal to the *Ulysses* counts times a factor of 0.63 (*straight line fit to the points*). The approximate fluences of the *Ulysses* bursts are indicated.

than that obtainable from the IPN alone. This includes events (cosmic or SGR) localized with X-ray cameras, and events with radio, X-ray, or optical counterparts. To date, 12 GRBs that meet one or more of these criteria, 5 bursts from SGR 1900+14, and 14 bursts from SGR 1806−20 have been used to verify *Odyssey's* timing and ephemeris. In these verifications, the triangulation is usually done using *Odyssey* and a near-Earth spacecraft, for which station-keeping is much simpler and more accurate, so that the timing and ephemeris uncertainties for this spacecraft are negligible.

When such events are triangulated, a "time shift" can be derived, which is the amount of time that would have to be added to the *Odyssey* time to obtain perfect agreement between the annulus derived from the *Odyssey* data and the known source position. This time shift is therefore a measure of the combination of statistical and systematic uncertainties in the triangulation. The statistical uncertainty depends only on the statistics of the two time histories that are being compared, and it is estimated in the cross-correlation analysis. The systematic uncertainty in these triangulations, which is a combination of timing and ephemeris errors, is always found to be much less than the statistical one. The latter varies between typical values of 1′ and 10′ (Fig. 5).

5. SOME SCIENTIFIC HIGHLIGHTS

5.1. *GRB 020405*

This event was observed by *Ulysses*, *Mars Odyssey*, Konus, and *BeppoSAX* (the GRBM experiment). The HEND and *Ulysses* time histories are shown in Figure 8. The first localization, to a 75 arcmin^2 error box, was produced within 16.6 hr (Hurley et al. 2002a). Multiwavelength observations of the afterglow were carried out by numerous ground- and space-based telescopes. An optical transient was identified in the error box (Fig. 9), and a redshift of 0.695 was found for it (Masetti et al. 2003). A bump in the optical afterglow light curve advanced the case for a supernova/GRB connection (Dado et al. 2002; Masetti et al. 2003; Price et al. 2003). Polarization studies of the optical afterglow were used to constrain the dust content of the host galaxy (Covino et al. 2003). Masetti et al. (2003) achieved the first detection of an afterglow in the NIR bands, and the first detection of a galaxy responsible for an intervening absorption line system in the spectrum of a GRB afterglow. Observations of a radio flare and of the X-ray afterglow were used to deduce the nature of the surrounding medium (Berger et al. 2003; Mirabal et al. 2003; Chevalier et al. 2004).

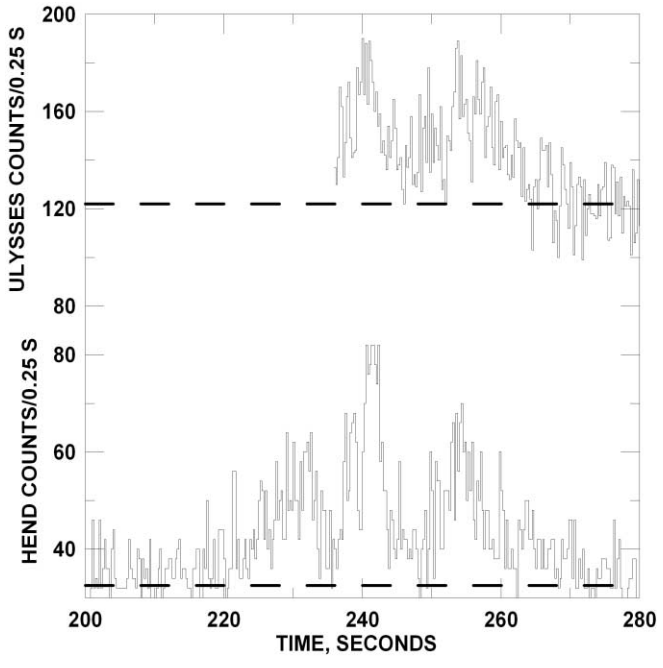

FIG. 8.—Time histories of GRB 020405, as detected by HEND and *Ulysses*. *Ulysses* triggered late in the burst.

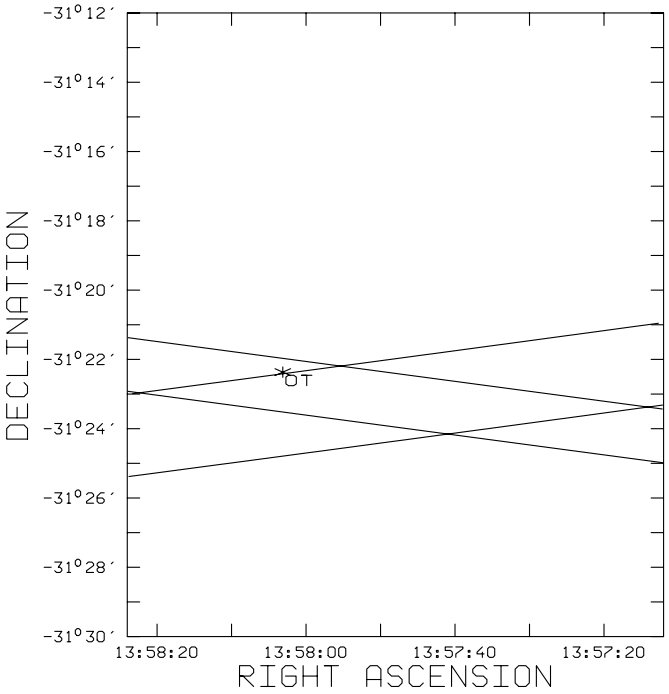

FIG. 9.—Final, 14 arcmin^2 IPN error box for GRB 020405, defined by the 2.′3 wide *Ulysses-Odyssey* and 1.′5 wide *Ulysses-BeppoSAX* annuli. The position of the optical transient detected by Price et al. (2003) is indicated.

5.2. *GRB 020813*

This event was observed by *Ulysses*, *Mars Odyssey*, Konus, and *HETE*. The *HETE* WXM and SXC produced localizations (Villasenor et al. 2002) that were used by Fox et al. (2002) to identify the optical counterpart, whose redshift was measured to be 1.2 (Price et al. 2002). The IPN error box had an area of 33 arcmin^2 and was circulated 24 hr after the burst (Hurley et al. 2002b, 2002c). It constrains the *HETE* positions, agrees with the optical position (Fig. 10), and serves both to verify them and to confirm the *Odyssey* timing and ephemeris.

5.3. *GRB 021206*

This event was detected by *Ulysses*, *Mars Odyssey*, Konus, *RHESSI*, and *INTEGRAL* (Hurley et al. 2002d, 2003). Polarization was detected in gamma-rays for this burst by *RHESSI* (Coburn & Boggs 2003; but see also Rutledge & Fox 2004 and Wigger et al. 2004), and the burst time history was used to set limits on the quantum gravity energy scale (Boggs et al. 2004). This event is a good example of the utility of the IPN technique. The IPN as a whole has isotropic response, and this burst occurred only 18° from the Sun. Thus, it is unlikely that it could have been detected and localized by *INTEGRAL*, *HETE*, or *Swift* due to pointing constraints. Since *RHESSI* is the only spacecraft that has a demonstrated polarization measurement capability, and it points in the

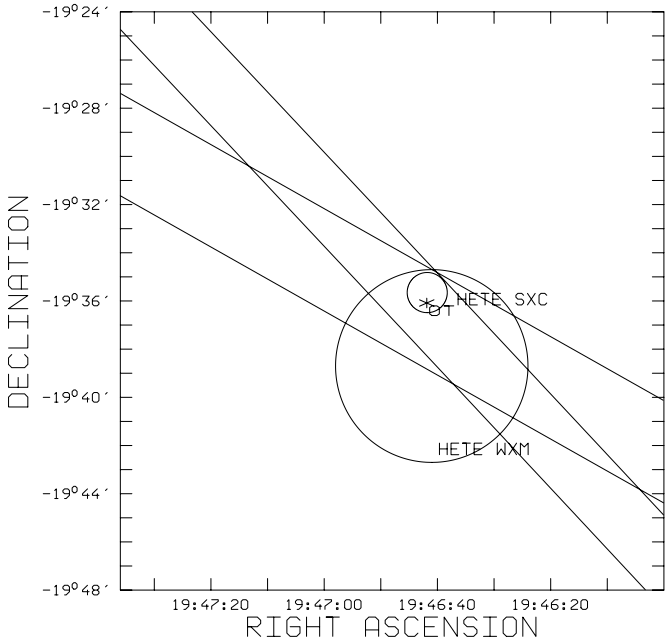

FIG. 10.—IPN and *HETE* localizations of GRB 020813. The IPN error box is defined by the intersection of the 2.′7 wide *Ulysses*-Konus annulus and the 3.′7 wide *Ulysses-Odyssey* annulus. The *HETE* WXM (Villasenor et al. 2002) and SXC Jernigan et al. (2002) error circles are shown for comparison. The position of the associated optical transient source (OT) found by Fox et al. (2002) is also indicated.

solar direction, only IPN-localized bursts can benefit from these measurements.

5.4. *The Giant Flare from SGR 1806−20*

An event that occurred on 2004 December 27 was the most intense burst of X-ray and gamma-radiation detected to date (Hurley et al. 2005; Gaensler et al. 2005; Palmer et al. 2005; Terasawa et al. 2005; Cameron et al. 2005). Although it was observed by at least 20 spacecraft, none of them could localize it. The precise localization, which was a key element in identifying the source, was done by triangulation using *Odyssey*. The burst turned out to be a giant flare from SGR 1806−20. This SGR was only about 5° from the Sun at the time of the burst.

6. CONCLUSIONS

The GSH and HEND experiments on board the *Mars Odyssey* spacecraft have been successfully integrated into the third interplanetary network. In this configuration, the IPN is producing rapid, precise GRB localizations at the expected rate, and should continue to do so for the foreseeable future. With the advent of newer missions such as *Swift* and *INTEGRAL*, with much greater sensitivities, and which are capable of independently determining GRB positions to better accuracies and with shorter delays, the question inevitably arises whether it is useful to maintain an IPN. There are several arguments in favor of this. The new missions achieve their accuracy and sensitivity at the expense of sky coverage; typically they view only 10%–20% of the sky, while the IPN is isotropic. Thus, first, the IPN serves as a continuous monitor of SGR activity throughout the galaxy, which the newer missions do not. And second, it will detect strong bursts at a rate that is 5–10 times greater than that of the newer missions. This makes it possible to study a wide variety of events that narrow field-of-view instruments will seldom detect. These include very intense bursts, very long bursts, repeating sources (gravitationally lensed GRBs and bursting pulsars like GRO 1744−28 are two examples), and possibly other as yet undiscovered phenomena. Two new missions, *Suzaku*, in low Earth orbit, and *MESSENGER* (*Mercury Surface, Space Environment, Geochemistry, and Ranging*), on a complex interplanetary trajectory to Mercury, are currently being added to the IPN. A second *Mars Odyssey* mission extension, from 2006 October to 2008 September, is currently under consideration. Therefore, the IPN should continue to serve a useful role in GRB and SGR studies for years to come.

We are grateful to John Laros for the initial work, which made GRB detection possible on board *Odyssey*. K. H. acknowledges support under the NASA Long Term Space Astrophysics and Odyssey Participating Scientist programs, FDNAG-5-11451.

REFERENCES

Berger, E., Soderberg, A., Frail, D., & Kulkarni, S. 2003, ApJ, 587, L5
Boggs, S., Wunderer, C., Hurley, K., & Coburn, W. 2004, ApJ, 611, L77
Boynton, W., et al. 2004, Space Sci. Rev., 110, 37
Cameron, P., et al. 2005, Nature, 434, 1112
Chevalier, R., Li, Z.-Y., & Fransson, C. 2004, ApJ, 606, 369
Coburn, W., & Boggs, S. 2003, Nature, 423, 415
Covino, S., et al. 2003, A&A, 400, L9
Dado, S., Dar, A., & De Rujula, A. 2002, A&A, 393, L25
Fox, D., Blake, C., & Price, P. 2002, GCN Circ. 1470, http://gcn.gsfc.nasa.gov/gcn/gcn3/1470.gcn3
Gaensler, B., et al. 2005, Nature, 434, 1104
Hurley, K., et al. 1999a, ApJS, 120, 399
———. 1999b, ApJS, 122, 497
———. 2002a, GCN Circ. 1325, http://gcn.gsfc.nasa.gov/gcn/gcn3/1325.gcn3
———. 2002b, GCN Circ. 1482, http://gcn.gsfc.nasa.gov/gcn/gcn3/1482.gcn3
———. 2002c, GCN Circ. 1483, http://gcn.gsfc.nasa.gov/gcn/gcn3/1483.gcn3
———. 2002d, GCN Circ. 1728, http://gcn.gsfc.nasa.gov/gcn/gcn3/1728.gcn3
———. 2003, GCN Circ. 2281, http://gcn.gsfc.nasa.gov/gcn/gcn3/2281.gcn3
———. 2005, Nature, 434, 1098
Jernigan, J. G., et al. 2002, GCN Circ. 1494, http://gcn.gsfc.nasa.gov/gcn/gcn3/1494.gcn3
Masetti, N., et al. 2003, A&A, 404, 465
Metzger, A., Boynton, W., Laros, J., & Trombka, J. 1992, in AIP Conf. Proc. 265, Gamma-Ray Bursts, ed. W. Paciesas & G. Fishman (New York: AIP), 353
Mirabal, N., Paerels, F., & Halpern, J. 2003, ApJ, 587, 128
Palmer, D., et al. 2005, Nature, 434, 1107
Price, P., Bloom, J., Goodrich, R., Barth, A., Cohen, M., & Fox, D. 2002, GCN Circ. 1475, http://gcn.gsfc.nasa.gov/gcn/gcn3/1475.gcn3
Price, P., et al. 2003, ApJ, 589, 838
Rutledge, R., & Fox, D. 2004, MNRAS, 350, 1288
Sagdeev, R., & Zakharov, A. 1990, Soviet Astron. Lett., 16, 125
Saunders, R., et al. 2004, Space Sci. Rev., 110, 1
Terasawa, T., et al. 2005, Nature, 434, 1110
Villasenor, J., et al. 2002, GCN Circ. 1471, http://gcn.gsfc.nasa.gov/gcn/gcn3/1471.gcn3
Wigger, C., Hajdas, W., Arzner, K., Gűdel, K., & Zehnder, Z. 2004, ApJ, 613, 1088
Ziock, K., et al. 1997, IEEE Trans. Nucl. Sci., 44, 1692